Enthalpy, Entropy, and Structural Relaxation Behaviors of A- and B-DNA in Their Vitrified States and the Effect of Water on the Dynamics of B-DNA

Simon Rüdisser, Andreas Hallbrucker, and Erwin Mayer*

Institut für Allgemeine, Anorganische und Theoretische Chemie, Universität Innsbruck, A-6020 Innsbruck, Austria

G. P. Johari*

Department of Materials Science and Engineering, McMaster University, Hamilton, Ontario L8S 4L7, Canada

Received: June 19, 1996; In Final Form: September 19, 1996[⊗]

The A and B forms of NaDNA with hydration level of between 0.15 and 0.64 (g of water)/(g of NaDNA) have been vitrified by cooling at rates between 4 and ∼2700 K min^{-1}, and their thermal behavior on reheating was studied from ∼120 to 300 K by differential scanning calorimetry (DSC). The effects of the annealing time, t_a, for two different hydration levels at a fixed temperature and of the annealing temperature, T_a, for a fixed t_a have been investigated, and the effects of various T_a and t_a on the enthalpy and entropy relaxations and recovery were ascertained. From these effects we evaluate τ_a, the characteristic structural relaxation time, E^*, the activation energy, τ_0, the preexponential factor, and $\beta < 1$ as an empirical parameter for apparent distribution of relaxation times. No DSC features of significance that may be attributed to the onset of molecular motions are found for A-DNA or when the water content is low, but for B-DNA and high water content, endothermic features resembling the onset of molecular motions, or glass → liquid transition, are observed from ∼153 K to ∼263 K. This corresponds to a slower increase in the heat capacity with temperature than is observed for most glass → liquid transitions, and it is attributed to the sum of a large number of relaxation modes of different parts with closely spaced single relaxation times. This is also seen as equivalent to a very broad distribution of structural relaxation times or of energy barriers separating the conformational and other substates corresponding to the various modes of local motions in a picture of multiple energy barriers. These local modes of motions involve both DNA segments and the water attached to them. Annealing vitrified B-DNA at temperatures from ∼153 K to ∼263 K causes its structure's net energy or enthalpy (and by implication its entropy) to decrease. The magnitude of this decrease has been measured by using the DSC difference scans in which the enthalpy lost on annealing is recovered on reheating but at a temperature higher than that of annealing. This recovered enthalpy increases with t_a according to the stretched exponential relation, $\Delta H(t_a) \propto 1 - \exp[-(t_a/\tau_a)^\beta]$. τ_a seems to remain constant with t_a but changes with T_a in much the same manner as for synthetic amorphous polymers. The peak temperature of the endotherm observed during the recovery of the lost enthalpy, T_p, also increases according to a relation, $T_p^2 \propto 1 - \exp[-(t_a/\tau_a)^\beta]$, with the same values of β and τ_a as for the increase in $\Delta H(t_a)$. It is concluded that the molecular segmental motions of B-DNA and of the water attached to it are attributable to a broad distribution of energy barriers between conformational substates.

Introduction

In DNA, dynamics is essential for its biological function and, as in proteins,[1,2] conformational substates seem to play a decisive role. Studies of DNA's dynamics and conformational substates have been made by a variety of techniques, e.g., by molecular dynamics calculations, X-ray diffraction, NMR spectroscopy, and dielectric relaxation, and refs 3−9 can be consulted for several reviews of the vast literature of this research area. We have recently reported a first study of DNA's dynamics by a further technique, namely enthalpy relaxation of vitrified NaDNA and its recovery on reheating by differential scanning calorimetry (DSC).[10] In this study we have investigated the effects of annealing temperature, T_a, annealing time, t_a, and hydration level, and we have shown that the calorimetric effects of T_a and t_a are characteristic of a glass. Structural relaxation became observable in the form of endothermic enthalpy recovery for $\Gamma > 3-4$ (water molecules per nucleotide), and the heat effects increased with hydration level linearly up to $\Gamma \approx 12$. These effects were attributed to the conformational flexibility of B-DNA. Here, we extend the previous study and quantify the calorimetric effects.

The dynamics of intra- and intermolecular motions in biologically active water-containing biomaterials is considered crucial to their activity. When such biomaterials are rapidly cooled from ambient to a sufficiently low temperature, e.g., from ∼300 to ∼100 K, most of the inter- and intramolecular or conformational modes of their motions become slower and ultimately too slow to be observable at an experimental time scale of, for example, 10^4 s. The biomaterial is said to have kinetically frozen, in many respects in a manner similar to that of vitrification of a liquid. During this occurrence all contributions to thermodynamic and molecular dynamic properties due to the conformational changes vanish at temperatures substantially below the glass → liquid transition temperature, T_g. At these temperatures only vibrational modes of motions, which are studied by measuring the Debye−Waller factor, are observed and their contribution to thermodynamic properties monotonically change only very weakly with temperature.

[⊗] Abstract published in *Advance ACS Abstracts,* December 15, 1996.

S1089-5647(96)01824-X CCC: $14.00

When the so-called vitrified or glassy material is heated, the magnitude of its thermodynamic properties, volume, enthalpy, and entropy increases rapidly with temperature once the configurational contribution to the property becomes detectable in the volume, enthalpy, and entropy measurements. This is observed as a seemingly discontinuous increase of the slope of the heat capacity, C_p, against temperature plot in an adiabatic measurement or more commonly as an increase in the heat input in a DSC experiment. For most glasses, including pure bulk water, the increase in the C_p or heat input becomes extremely rapid at a certain temperature and the resulting shape of the C_p or heat input against temperature curve becomes a sigmoid. When such experiments are done with hydrated proteins such as myoglobin, hemoglobin, and lysozyme,[11] or with cytochrome *c* and poly-L-asparagine,[12] no discontinuous increase in C_p or heat input is found and thus no rapid change in the thermal properties that can be attributed to the onset of configurational contribution, or T_g endotherm, is observed. When the myoglobin crystal contained 22 wt % NaH_2PO_4, 27 wt % K_2HPO_4 from the buffer solution,[13] sharp sigmoid-shaped endotherms were observed on heating. But these endotherms are attributable to the glass transition characteristic of the freeze-concentrated buffer solution.[11] Thus, the absence of the usual glass transition endotherm in calorimetric studies of proteins has led to doubts as to what temperature proteins truly vitrify and whether measurements by X-ray, neutron, and other diffraction techniques could be associated with the calorimetric glass → liquid transition due to segmental motions of the protein macromolecule.[14]

Sartor et al.'s study[11] has now resolved this issue. They developed an anneal-and-scan procedure using DSC, a technique that Breslauer et al.[15] consider as one of the most revealing for the dynamics of molecular motions and of thermodynamics for DNA and ligand−DNA studies. In order to clearly demonstrate that the endotherms observed for three hydrated proteins, hemoglobin, myoglobin, and lysozyme, on anneal-and-scan experiments are due to the recovery of the enthalpy that was lost during the isothermal annealing, Sartor et al.[16] also studied a dry interpenetrating network polymer, which showed a featureless DSC scan, i.e., an increase in C_p over a broad temperature range similar to that observed for the hydrated proteins. The conclusion of their study was that in its anneal-and-scan DSC features the synthetic polymer mimicked the proteins, indicating that in proteins the distribution of modes of molecular motions is exceptionally broad and that the DSC features transcend the details of well-known (and obvious) structural differences between the hydrated proteins and the dry network polymer. Thus, it seemed that the physical justification, in terms of the nature of molecular kinetics, of Kuntz and Kauzmann's[17] original thoughts where protein solutions may be interpreted as polymer solutions is rooted in the physics of molecular kinetics and not, as is occasionally believed, in the chainlike, cross-linked, or helical configurational nature of the polymer or macromolecule. This anneal-and-scan procedure has now been successfully used by Green et al.[12] for revealing the configurational changes and thus establishing the vitrification characteristics of cytochrome *c* solution.

In this paper, we use the above-mentioned anneal-and-scan DSC studies to show that B-DNA containing varying amounts of water has a broad distribution of intra- and intermolecular relaxation times that, as for proteins, become evident as a broad endotherm. We further develop these ideas in mathematical terms and discuss how the enthalpy lost on isothermal annealing (also referred to as physical aging) and recovered on heating changes with t_a and how the peak temperature of the endothermic peak observed when enthalpy is regained changes with t_a.

Apart from giving a direction in which calorimetry can be used further in studies of DNA and other biomaterials, the studies reported here show how hydrated DNA becomes molecularly mobile (within an observation period of $\sim 10^4$ s) at a certain temperature and how the physics of these processes may be formulated. We hope that similar DSC studies in the future would be able to identify the various parts of the DNA molecule that become active at subambient temperatures, how local energy barriers to various conformational substates can be found for each repetitive nucleotide, and how the population of the various conformational substates or the local energy balance between substates corresponding to a base sequence is disturbed by long-range effects when dipolar and other interactions become more important on decreasing the thermal energy.

Other studies of the dynamics of DNA at low temperatures, for example, by calorimetry,[18] thermally stimulated depolarization currents,[19,20] and Rayleigh scattering of Mössbauer radiation,[21] have been reported, but these studies were not done in the same manner as shown here, by investigating enthalpy loss and its recovery via our anneal-and-scan method.

Experimental Section

The sodium salt of DNA from salmon testes, NaDNA, was obtained from Fluka Chemical Co. (No. 31163). As-received NaDNA contained according to its specification 12.9 wt % water and 0.08 wt % protein. Its water content was confirmed by measurements. NaDNA was hydrated by keeping it over saturated salt solutions for several weeks and the water content determined by weighing to ±0.01 mg, taking into account the water content of the as-received NaDNA. The hydrated samples were quickly transferred into steel capsules, or for the DSC scans of Figure 5, into aluminum pans. The weights of the samples were between about 10 and 40 mg. The accuracy of the given hydration values is estimated to be ±0.02 (g of water)/(g of dry NaDNA). In one case (not shown) a sample obtained by hydration of as-received NaDNA solution was compared with a sample obtained by dehydration of an aqueous NaDNA solution, keeping both over saturated $(NH_4)_2SO_4$. Identical DSC results were obtained from both samples.

NaDNA was characterized further by FTIR spectra of a NaDNA film on AgCl disk, which was hydrated either at 93% relative humidity (r.h.) (over KNO_3 solution) or at 54% r.h. (over $Mg(NO_3)_2$ solution). A comparison with FTIR spectra reported by Taillandier et al.[22] in their Figure 2 showed that the spectral features of hydration at 93% are those of the B form and those of hydration at 54% are those of the A-form. This is consistent with the reported change in A- and B-conformer population with hydration level.[8,23−27] The hydration levels between 0.19 and 0.64 (g of water)/(g of NaDNA) used for the DSC scans of Figure 1 correspond to hydration values between 40 and 82% relative humidity (read from Figure 1 in ref 23).

A differential scanning calorimeter (Model DSC-4, Perkin-Elmer) with a selfwritten computer program was used for all studies. After the scans were taken, a base line obtained with empty sample pans was subtracted to eliminate curvature of the scans. In addition, a straight line was subtracted from each DSC scan, with set points placed at ∼110 and ∼130 K. This is equivalent to slope control in the original software. The data were imported into Origin, a computer program used to prepare the plots (MicroCal Software). The samples were cooled in the DSC instrument at a rate of ∼80 K min^{-1} unless noted otherwise. The DSC scans were recorded on heating from 103 to 298 K at a rate of 30 K min^{-1}. For investigation of the effect

of annealing, the samples were heated from 103 K to the given annealing temperature, kept at this temperature for a given annealing time, and cooled thereafter to 103 K at 30 K min^{-1} for heating and recording the DSC scan. The difference curves were obtained by subtracting the scan of an unannealed sample from that of the same sample but annealed in addition at the given temperature. The temperature scales in Figures 1−4 and 6, where original DSC scans or difference curves are shown, are not corrected for thermal lag of the instrument (which is 1.6° for heating at 30 K min^{-1} for steel capsules). However, the temperature scales of the other figures and temperatures given in the text are corrected for thermal lag. The DSC scans of each figure are normalized with respect to the samples' weights but shifted vertically for clarity. The ordinate bar is for 1 mg of hydrated NaDNA. References for further experimental details on DSC and cooling rates are given in refs 11 and 28.

Steel capsules with screwable lids were preferred in this study to the crimp-sealed aluminum pans used before[11] because we observed that for the same hydrated NaDNA sample, the noise and the change of slope are less when using steel capsules rather than aluminum pans. This is best seen in difference curves obtained by subtracting two DSC scans recorded immediately one after the other and by the comparison of such difference curves obtained by using either steel capsules or aluminum pans with similar sample weight and with the sample taken from the same batch. Increased signal-to-noise ratio is attributed to better thermal contact between the sample pan and the instrument cup for steel capsules than for aluminum pans. Thermal contact is a well-known problem for DSC measurements,[29] and one way to improve thermal contact between the sample pan and the instrument cup is to apply silicone grease between the pan and the cup. This is obviously not meaningful for measurements at subambient temperature because of the intense glass transition endotherm of silicone grease. Evaporation losses were minimized by heating at most up to 303 K and by cooling immediately after reaching that temperature. Evaporation losses were determined by reweighing the sample and steel capsule after the DSC measurements, and weight loss was at most 2 wt % of the water fraction. This is less than the error of ±0.02 (g of water)/(g of NaDNA) given for the hydration level. Crimp-sealed aluminum pans were used only for the scans of Figure 5 because of the high cooling rates obtainable.[28]

Results

Figure 1a shows DSC scans of four unannealed (scans 1−4) and annealed (scans 1′−4′) samples of NaDNA containing increasing amounts of water. For scans 1−4, the samples were cooled from 298 to 103 K at a rate of ∼80 K min^{-1} in the DSC instrument, stabilized isothermally at 103 K, and thereafter heated to 298 K at a rate of 30 K min^{-1} and their DSC scan recorded. DSC scans obtained for empty pans have already been subtracted from the scans of the sample-containing pans. Scan 1 is for a sample containing 0.19 (g of water)/(g of NaDNA) and scans 2−4 are for samples containing 0.29 (2), 0.45 (3), and 0.64 (4) (g of water)/(g of NaDNA), respectively. The DSC output for curve 1 shows a very gradual increase with increasing temperature and no indication of a rapid rise that may be attributed to the onset of molecular motions. For water in the amount of 0.29−0.64 (g of water)/(g of NaDNA) in curves 2−4, the DSC output shows a sigmoid shape caused by an increase in slope at about 175−200 K and a decrease in slope at about 240−275 K. This sigmoid shape is modified in scan 4 by the presence of an endotherm attributed to the melting of ice. In scans 2−4 the sigmoid is spread from ∼175−200 up to ∼240−275 K, which is too broad to be attributed to a glass transition in most materials. The plateau region seen in scans 3 and 4 above ∼240 K might not be real because a straight line has been subtracted with set points at ∼110 and ∼130 K, which is equivalent to a change of slope of the whole curve, but the decrease in slope above ∼240 K is real.

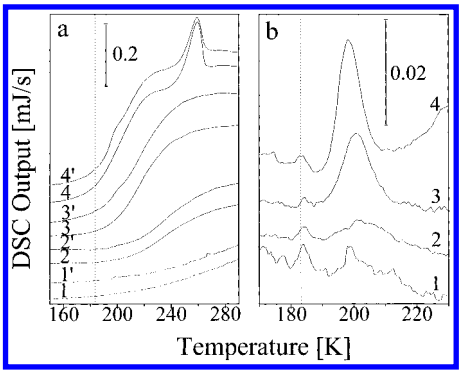

Figure 1. Effect of hydration level and of annealing increasingly hydrated NaDNA as seen in DSC scans obtained during heating at 30 K min^{-1}: (a) scans 1−4 are for NaDNA samples containing 0.19 (1), 0.29 (2), 0.45 (3), and 0.64 (4) (g of water)/(g of NaDNA), respectively, and scans 1′−4′ are for the same samples that have been annealed for 20 min at 183 K (broken line) before recording the DSC scans; (b) DSC difference curves obtained by subtracting the scan of an unannealed sample (scans 1−4) from that of the same sample but annealed for 20 min at 183 K (scans 1′−4′), i.e., difference curve 1 is obtained by subtracting scan 1 from scan 1′. The broken line is at 183 K (from ref 10 with changes).

For the study of the characteristics of the very broad endotherm observed, each sample was annealed at a fixed temperature of 183 K for a fixed period of 20 min. In this procedure the sample was cooled from 298 to 103 K at ∼80 K min^{-1}, thermally equilibrated at that temperature, heated to 183 K at 30 K min^{-1}, kept at 183 K for 20 min, cooled thereafter to 103 K at 30 K min^{-1}, equilibrated at 103 K, and finally heated to 298 K at 30 K min^{-1} and its DSC scan recorded. Figure 1a also shows the DSC scans thus obtained, where the numbering 1′−4′ refers to scans 1−4 of the same samples but annealed in addition. In curves 2′−4′ a weak endothermic feature was observed above T_a for all samples containing from 0.29 to 0.64 (g of water)/(g of NaDNA), which seems to be superposed on the shape of the corresponding scans of the unannealed samples and which is clearly evident at higher hydration level in scans 3′ and 4′.

The above-described anneal-and-scan method thus reveals the molecular kinetic effects implicit in the shape of the DSC curves, as in earlier studies of hydrated NaDNA[10] and of hydrated lysozyme, hemoglobin, and myoglobin.[11] More importantly, it allows us to examine the anneal-and-scan effects in a quantitative manner by determining the difference between the two scans for the same sample of hydrated NaDNA, as given in Figure 1a. This difference is plotted against the temperature in Figure 1b where the labeling of the curves 1−4 refers to the same sample as in Figure 1a, i.e., difference curve 1 was obtained by subtracting scan 1 from scan 1′ from Figure 1a. In Figure 1b, curves 2−4 show an endothermic peak whose area increases with increasing hydration level and whose peak temperature decreases from 201.3 K for curve 2 to 196.5 K for curve 4. This endothermic feature, with an extrapolated peak temperature of 205 K, is absent in curve 1. In curve 1 weak endothermic features at, for example, 183 and 198 K, are attributed to noise, the relatively large distortion or noise in this curve being a result of the fact that two DSC scans, each with weak features and small DSC outputs, were subtracted from each other. This noise becomes less with increasing hydration

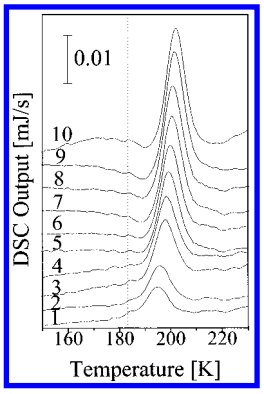

Figure 2. DSC difference curves of hydrated NaDNA containing 0.53 (g of water)/(g of NaDNA) obtained by annealing at a fixed temperature of 183 K for various annealing periods. The same sample was used throughout. The annealing time for curves 1−10 is 1, 2, 7, 10, 20, 28, 46, 59, 105, and 113 min, respectively.

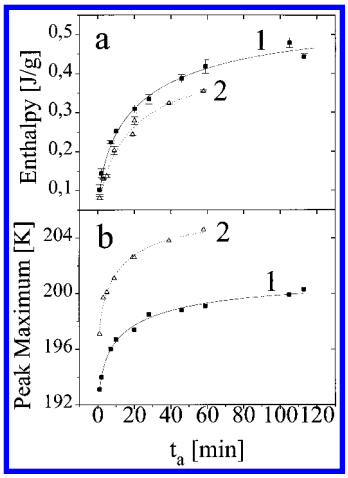

Figure 3. Plots of (a) recovered enthalpy in J/(g sample) and of (b) peak maximum versus annealing time, labeled 1, for NaDNA containing 0.53 (g of water)/(g of NaDNA) (values are from Figure 2). The corresponding plots for NaDNA containing 0.48 (g of water)/(g of NaDNA) are labeled 2. The samples were annealed at 183 K for various annealing times.

in curves 2−4, which has to do with the increased sample amount and possibly with improved thermal contact between the sample and the pan with increasing hydration.

The change in the endothermic peak area with t_a for a fixed amount of water was then investigated, and for this purpose a sample containing 0.53 (g of water)/(g of NaDNA) was chosen. The difference curves of the DSC output in Figure 2 were determined as for the samples shown in Figure 1b by subtracting the scan of the unannealed sample from that of the annealed sample. For the purposes here, the sample was cooled from 298 to 103 K at ∼80 K min^{-1}, equilibrated at 103 K, heated to 183 K, and kept at 183 K for increasing annealing periods: 1 min for curve 1 and 2, 7, 10, 20, 28, 46, 59, 105, and 113 min for curves 2−10, respectively. Thereafter, the sample was cooled from 183 to 103 K at 30 K min^{-1} and the DSC scan obtained on heating from 103 to 298 K at 30 K min^{-1}. For clarity, only the 150−230 K part of the difference curves is shown in Figure 2 here. The broken line marks T_a. Curves 1−10 in Figure 2 clearly show that the height of the endothermic peak increases and its position shifts toward higher temperature as t_a is increased. This endothermic feature is absent in the unannealed sample (not shown). In Figure 3, the integrated areas of the endothermic peaks shown in Figure 2 and their peak temperatures are plotted versus t_a, and the data points are labeled as curve 1. Figure 3 further contains as curves two

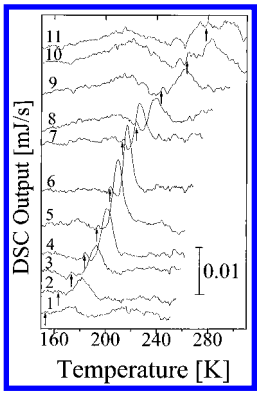

Figure 4. DSC difference curves for demonstrating the influence of annealing temperature for constant annealing time of 20 min. The same sample containing 0.46 (g of water)/(g of NaDNA) was used throughout. The annealing temperatures are 153 (1), 163 (2), 173 (3), 183 (4), 193 (5), 203 (6), 213 (7), 223 (8), 243 (9), 263 (10), and 278 K (11), and these temperatures are marked by the arrow.

data points of a second NaDNA sample containing 0.48 (g of water)/(g of NaDNA) for the same T_a of 183 K and for t_a up to 58 min.

To investigate the effect of T_a, a sample containing 0.46 (g of water)/(g of NaDNA) was annealed at different annealing temperatures for a constant t_a of 20 min. Figure 4 shows difference curves of the DSC output that were determined in the same manner as those shown in Figures 1b and 2, by subtracting the scan of the unannealed sample from that of the annealed sample. For the purposes here, the sample was cooled from 298 to 103 K at ∼80 K min^{-1}, equilibrated at 103 K, heated to T_a, and kept at T_a for 20 min. Thereafter, the sample was cooled to 103 K and finally reheated to 298 K and its DSC scan recorded. The annealing temperatures are 153 (1), 163 (2), 173 (3), 183 (4), 193 (5), 203 (6), 213 (7), 223 (8), 243 (9), 263 (10), and 278 K (11), and these temperatures are marked by the arrows.

In cryopreservation processes, samples of DNA and other biological materials are usually cooled at a rapid rate. The DSC scans obtained on heating such samples differ from those obtained for slowly cooled samples, as do the annealing effects, even when formation of ice can be avoided by using cryoprotectants or low hydration level. To examine this effect for hydrated DNA, a sample containing 0.50 (g of water)/(g of NaDNA) was cooled at different cooling rates from 298 to 103 K, equilibrated at 103 K, heated at 30 K min^{-1} to 183 K, annealed for 65 min, and cooled at 30 K min^{-1} to 103 K. Finally, the sample was heated from 103 to 298 K at 30 K min^{-1} for recording the DSC scan. These scans are shown in Figure 5a. Scans 1−4 are for the unannealed samples, and scans 1′−4′ are for the annealed samples. The cooling rates are 4 (1, 1′), ∼150 (2, 2′), ∼1500 (3, 3′), and ∼2700 K min^{-1} (4, 4′). The difference curves in Figure 5b were obtained by substracting the scan of an unannealed sample from that of the same sample but annealed for 65 min at 183 K.

Discussion

1. General Aspects. Before discussion of the large number of accurate results obtained by varying T_a, t_a, the hydration level, and the cooling rate as seen in Figures 1−5, it seems necessary that basic elements of the dynamics of conformational (related to the secondary, tertiary, and quaternary structures when thermally induced reversible changes in the local structure involve overcoming *intra*molecular barriers for rotation about the covalent bonds of the DNA molecule) and configurational (in a statistical−thermodynamical sense when the thermally

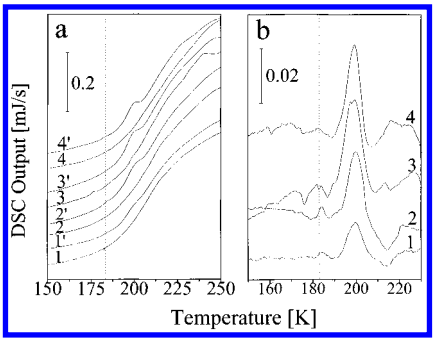

Figure 5. DSC curves demonstrating the influence of cooling rate on recovered enthalpy. (a) The DSC scans of hydrated NaDNA with 0.50 (g of water)/(g of NaDNA) were recorded on heating, after cooling from 298 to 103 K at the following cooling rates: 4 (scans 1 and 1′), ∼150 (scans 2 and 2′), ∼1500 (scans 3 and 3′), and ∼2700 K min^{-1} (scans 4 and 4′). Scans 1−4 are for unannealed samples. For scans 1′−4′ the samples were annealed at 183 K for 65 min. (b) The influence of the cooling rate is shown in form of difference curves (i.e., annealed − unannealed scans of Figure 5a). Curve 1 is scans 1′−1 of Figure 5a for cooling at 4 K min^{-1}. Curve 2 is scans 2′−2 for cooling at ∼150 K min^{-1}. Curve 3 is scans 3′−3 for cooling at ∼1500 K min^{-1}, and curve 4 is scans 4′−4 for cooling at ∼2700 K min^{-1}.

induced changes in the local structure involve overcoming *inter*molecular barriers for bodily motions of water molecules and the DNA's segments) freezing and unfreezing be outlined. It must be stressed that conformational dynamics occurs in an environment in which intermolecular barriers predominante, and so the conformational and configurational dynamics become coupled, with the latter dominating in a condensed system. Here, in addition, a chemically distinguishable isomeric state of DNA may form as a result of conformational changes, and this new state may even become more stable at a certain temperature than any other conformational state. Such an occurrence would be equivalent to a chemical change if that conformational isomeric state can perform a chemical function different from those of the remaining conformational states, as well as be characterized by other physical methods. Thus, a change in the thermal energy is expected not only to produce different conformational and configurational substates but also to produce a distinct and characterizable chemical isomeric state. The latter, once identified as a distinct substance, may have its own set of conformational and configurational substates.[1,2]

When a sample of dry or hydrated DNA is cooled at a certain rate, the various conformational degrees of freedom of its glycophosphate chain, of the H-bonded nucleotides, and of the H-bonded water molecules in it become progressively less accessible as the configurational kinetics becomes slower and its rate becomes ultimately comparable to the rate of cooling. Thus, if the hydrated DNA was to have a total of n number of conformational and rotational degrees of freedom available at ambient temperature, all contributing to its configurational heat capacity, C_p(conf), enthalpy, H, and entropy, S, then on cooling of the hydrated DNA, the number of such degrees of freedom will become less than n, decreasing to virtually zero at a temperature when no conformational dynamics is possible within a time scale of $\sim 10^4-10^5$ s. As a consequence, the configurational C_p vanishes, but the configurational H and S become frozen in and therefore remain finite and their magnitude corresponds to the configurational H and S of that conformational or other dynamical mode that became frozen in at a certain temperature.

The thermodynamic state of hydrated DNA becomes metastable with respect to only those degrees of freedom that are kinetically frozen in. When the vitrified sample is heated at the same rate, the same conformational degrees of freedom become available at the same temperature at which they were kinetically frozen in and configurational C_p, H, and S increase with temperature. When the number of such degrees of freedom n is small or the apparent distribution of relaxation times is narrow, the shape of the C_p vs temperature plot or of the DSC scan is a sharp sigmoid. This is observed for most synthetic organic polymers and inorganic glasses where the usual glass transition temperature, T_g, can be determined. But when n is very large or the apparent distribution of relaxation times very broad, the shape of the DSC scan becomes extremely broad and the T_g is neither easily determined nor meaningful. In such cases, as for hydrated DNA here[10] and for hydrated lysozyme, hemoglobin, and myoglobin,[11] it becomes necessary to consider each conformational and configurational dynamic mode as its own *mini* glass transition endotherm and the overall shape of the DSC scan as a weighted average of these n number of *mini* glass transition endotherms spread over a broad temperature range. The shape of the DSC scan may resemble the shape obtained for a broad continuous distribution of relaxation times but may not exactly match it unless the distribution itself is allowed to change with temperature. The very broad sigmoid shapes of the DSC scans seen in Figure 1a may be approximately interpreted as either the sum of n *mini* glass transitions or as a broad distribution, with the distribution itself changing with temperature. This was briefly pointed out in earlier papers.[10,11]

As vitrified hydrated DNA is annealed at a certain temperature, its thermodynamic state irreversibly relaxes toward equilibrium. This is a consequence of molecular or segmental mobility of hydrated DNA that occurs during annealing and allows some of the conformational and configurational states to reach their low-energy thermodynamic equilibrium. In this process, heat is evolved or the enthalpy decreases and the frozen in configurational entropy associated with the frozen in conformational and configurational states is lost.

The decrease in H and S on annealing thus becomes an indication of the mobility in the vitrified state of hydrated DNA, and the magnitude of this decrease becomes an approximate measure of the number of conformational and configurational modes whose dynamics contributes to the loss of H and S. There are several review articles on the annealing, or physical aging, behavior of vitrified solids (excluding biopolymers), which describe a procedure for mathematical modeling of the annealing effects in synthetic organic polymers and inorganic glasses. These are meant for cases where the glass transition endotherm is sharp, and such modeling requires that arbitrary and independently untestable values of four parameters be used until the calculated DSC scan approximately coincides with the measured scan. This modeling also requires that C_p of the substance in the thermodynamic equilibrium state remains constant over the whole modeled temperature range. Details of the procedure for such modeling are given in refs 30−37. The approximation of constant C_p becomes even more severe here in view of the broadness of the features. For discussing the results of hydrated DNA, we therefore use a phenomenological or physical approach as is relevant to our experiments and not the mathematical modeling used for synthetic polymers and inorganic glasses.

2. Formalism. The irreversible total decrease in enthalpy on annealing, ΔH_a, may be written as

$$d\Delta H_a = \left(\frac{\partial \Delta H_a}{\partial t_a}\right)_{w,T_a} dt_a + \left(\frac{\partial \Delta H_a}{\partial T_a}\right)_{w,t_a} dT_a + \left(\frac{\partial \Delta H_a}{\partial w}\right)_{t_a,T_a} dw \quad (1)$$

where ΔH_a is the difference between the enthalpy before and

after the annealing experiment, t_a the annealing time, T_a the isothermal temperature of annealing, and w the amount of water in DNA. The first term on the right-hand side represents the enthalpy loss (or decrease) with respect to time at constant w and T_a, as in isothermal annealing. The second term represents the enthalpy loss with respect to temperature at constant w and t_a, and the third term represents the enthalpy loss with respect to the amount of water in DNA for a constant t_a and T_a. The curves in Figure 2 show the effects represented by the first term, those in Figure 4 the effects represented by the second term, and those in Figure 1 the effects represented by the third term.

The corresponding total decrease in entropy, ΔS_a, may be written as

$$d\Delta S_a = \left(\frac{\partial \Delta S_a}{\partial t_a}\right)_{w,T_a} dt_a + \left(\frac{\partial \Delta S_a}{\partial T_a}\right)_{w,t_a} dT_a + \left(\frac{\partial \Delta S_a}{\partial w}\right)_{t_a,T_a} dw \quad (2)$$

where the terms have the same meaning as in eq 1.

It should be noted that the first term of eqs 1 and 2 represents a physical process at temperatures below ~220 K, since it is a measure of the dynamics of segments of a molecule or of molecules themselves in a certain potential energy environment. (Reasons as to why the contributions from a possible chemical reaction involving an exothermic conformational change should be negligible or zero for hydrated DNA below ~220 K are given in section 7. The features of the difference curves obtained at higher temperatures will be discussed separately in the same section.) The second and third terms represent effects that are due partly to a chemical process and partly to a physical process. They represent a chemical process when a change in temperature stabilizes, according to the second term, one chemically distinct and physically characterizable isomeric structure over the other and when a change in the hydration level alters, according to the third term, the chemically distinct isomeric state of the DNA molecule itself. The second and third terms represent a physical process when changes in the temperature and hydration level control the dynamics of the various segments and domains in the entire system, once the chemically distinct isomeric structure has formed, by the new potential energy hypersurface corresponding to that distinct isomeric structure of the DNA.

It is useful to explain the physical meaning of eqs 1 and 2 as follows. Suppose a hydrated DNA or protein sample is stored at ~200 K, a temperature in which some of its segments are mobile and others are kinetically frozen in, in a gaseous environment to which it could lose water or from which it could absorb water, and suppose that the temperature of the entire system fluctuates over time. The total loss of the enthalpy and entropy of the sample can be calculated from eqs 1 and 2. However, if the molecular dynamics that allows the enthalpy and entropy decrease under these conditions involves DNA or protein segments that can react with the water vapor present in the environment, the reaction between the DNA or protein and water vapor will occur, leading to a change, and eqs 1 and 2 will no longer apply.

In the following sections we examine our experimental results within the context of eqs 1 and 2 and provide formalisms for each of the three terms and for their relevant features, as obtained by DCS here. In section 7 we provide the implication of these thermodynamic and kinetic effects for the studies of DNA and proteins and other biological materials.

3. Effect of the Annealing Time. The data labeled 1 in Figure 3 are obtained from Figure 2, and they yield information on the decrease in enthalpy and entropy on annealing a sample containing 0.53 (g of water)/(g of NaDNA) at a fixed temperature, or information on the first term of eqs 1 and 2. The integrated area of the endothermic peak is equal to the enthalpy lost on isothermal annealing plus any further and negligible loss that could occur on heating the sample from T_a until the onset temperature of the endothermic peak, which is being integrated. The latter can only be small because there is no observable exothermic dip in curves 1−6, and hence, the total enthalpy obtained by integrating, or the enthalpy gained on heating, is equal to the enthalpy lost on isothermal annealing. This is a well-established observation and has been widely used[37−39] and reviewed by Hodge[29] for studying the vitrified states of several polymers and of molecular and inorganic materials. Curves 7−10 show above T_a a weak dip in C_p, or equivalently in the calorimetric output, immediately before the endotherm. Similar dips have been observed in DSC curves of polymeric and metallic glasses and attributed to the so-called memory effect.[29]

The loss of enthalpy on isothermal annealing calculated from the area of the endotherm is plotted against the annealing time as curve 1 in Figure 3a. The data points were obtained for isothermal annealing of a sample containing 0.53 (g of water)/(g of NaDNA) at 183 K up to 113 min. The continuous line through the data points for the enthalpy loss, $\Delta H_a(t_a)$, was calculated from the equation

$$\Delta H_a(t_a) = H(0) - H(t_a) = \Delta H_a(\infty)[1 - \exp(-(t_a/\tau_a)^{\beta})] \quad (3)$$

where t_a is the annealing time, τ_a the characteristic time for the molecular process that causes annealing, β an empirical parameter with a value between zero and 1, which is independent of t_a, $H(0)$ the enthalpy at the beginning of annealing, i.e., at $t_a = 0$, $H(t_a)$ the enthalpy after a period t_a, and $\Delta H_a(\infty) = H(0) - H(\infty)$, where $H(\infty)$ is the enthalpy as $t_a \rightarrow \infty$. Equation 3 represents a stretched exponential increase in $\Delta H_a(t_a)$ with t_a when $\beta < 1$. The smooth line in curve 1 of Figure 3a is shown for $\beta = 0.5$, $\tau_a = 25$ min, and $\Delta H_a(\infty) = 0.53$ J/(g sample). A similar method for evaluating these parameters has been described by Mountain and Thirumalai.[40] The accuracy of the given β value is ±0.1 and the accuracy of the given τ_a value ±5 min. For $\Delta H_a(\infty)$ it is ±0.04 J/(g sample).

Figure 3b shows as curve 1 the plot of the peak temperature of the endotherm, T_p, versus t_a. Rapid increase of T_p at short t_a and its leveling off at long t_a is a characteristic for enthalpy relaxation of a glass and its recovery.[29] The smooth line in curve 1 of Figure 3b was calculated according to the equation $T_p(t_a) = 187.3 + 13.52(\Delta H_a(t_a))^{1/2}$, which was obtained from eq 4.

Plotted on a logarithmic scale of t_a, the plot of $\Delta H_a(t_a)$ does not have a sigmoidal shape as implied by eq 3 (see Figure 7a). This indicates that equilibrium has not been reached yet. During the annealing of a sample containing 0.53 (g of water)/(g of NaDNA), water molecules and only those segments of the DNA molecule whose relaxation time lies within the time range of τ_a rearrange conformationally and/or configurationally and reach their lowest energy equilibrium state and the enthalpy decreases. Within the period of t_a, the contribution may be partly due to partial relaxation of those segments that have either begun to relax and have not reached their limiting low-energy state (in this case the enthalpy lost corresponds to a value from $H(0)$ to $H(t_a)$) or have partially already relaxed (in this case the enthalpy lost corresponds to the amount released as the limiting low-energy $H(\infty)$ is approached). The characteristic relaxation time, τ_a, of 25 min for a sample containing 0.53 (g of water)/(g of NaDNA) formally represents an average value. Its relation with the segmental motions can be understood only by a suitable analysis of the apparent distribution of relaxation times.

Figure 3 further contains data points of a second NaDNA sample containing 0.48 (g of water)/(g of NaDNA), which are

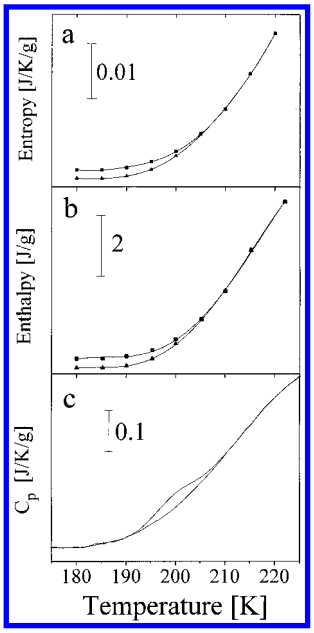

Figure 6. In (c) the heat capacity of NaDNA containing 0.52 (g of water)/(g of NaDNA) is shown for the annealed and the unannealed sample. The annealing time was 20 min at 183 K. (b) The upper curve shows the enthalpy of the unannealed sample, and the lower curve shows the enthalpy of the annealed sample obtained by integration of the C_p curves in (c). (a) The entropy of the unannealed sample (upper curve) and the annealed sample (lower curve) was obtained by integration of C_p/T versus T curves.

labeled as curve 2. For a given t_a, the enthalpy is lower and the peak temperature higher for the data points of curve 2 than for those of curve 1. This is consistent with a decreasing mobility with a decrease in hydration level. The broken lines of curve 2 were obtained for $\beta = 0.6$, $\tau_a = 19$ min, and $\Delta H_a(\infty) = 0.41$ J/(g sample), with the same estimates for accuracy as for curve 1. Results from a comparison of curve 1 with 2 seem to be in contradiction to the general observation that for a given sample with increasing t_a, an increase in recovered enthalpy is accompanied by an increase in peak temperature.[30,41] However, here we compare the effect of t_a on two NaDNA samples of different hydration levels and, by implication, different mobility.

In parts a and b of Figure 6, the recovery of the enthalpy and entropy on heating shows a more rapid increase in H and S for the annealed sample (lower curve) than for the unannealed one (upper curve). The original DSC scans for this figure were obtained with a sample containing 0.52 (g of water)/(g of NaDNA), and the sample was annealed at 183 K for 20 min. The enthalpy scale in Figure 6b was obtained by integration of Figure 6c. The slope of both C_p curves in Figure 6c has been set to zero between 175 and 180 K by substracting a straight line from the C_p curves. It is probably justified to assume the same C_p value and the same slope of the C_p versus T curve below T_a for both the unannealed and the annealed sample. Therefore, substraction can influence the magnitude of the increase in the H versus T curves in case the slope of the C_p versus T curves is nonzero between 175 and 180 K. But the relative H values of annealed versus unannealed are not affected by this procedure. The same argument holds for the entropy scale.

Although it now seems uncertain as to what specific modes of motions allow the loss and regain of H and S, the discussion in section 7 explains how insight into these motions in DNA can be gained. The plots of Figure 3 represent a typical behavior of the hydrated DNA sample when it is isothermally annealed and when the availability of the equilibrium conformational states at that temperature slowly reduces its enthalpy and entropy. When it is heated, the availability of new equilibrium conformational states as a result of the increase in thermal energy kT allows the recovery of the enthalpy and entropy. This is completed at a temperature where in parts a and b of Figure 6 the two curves meet.

One more aspect of the anneal-and-scan features needs to be considered. Although this aspect may seem entirely phenomenological, it is undoubtedly relevant to both this study of DNA[10] and the earlier study of proteins.[11] When DNA is heated, the peak observed in the DSC output, or equivalently the C_p endotherm, moves to a higher temperature when t_a is increased as shown in Figure 2 for a sample containing 0.53 (g of water)/(g of NaDNA), and this peak temperature appears to reach a limiting value. This is more clearly seen in plot 1 of Figure 3b. Concommitant to this, the area under the peak or the total enthalpy lost on annealing, or recovered on heating, increases and reaches a limiting value as described earlier in this section and shown in plot 1 of Figure 3a for the same sample containing 0.53 (g of water)/(g of NaDNA). If the relaxation time τ_a for molecular motions that lead to the annealing processes were to follow an Arrhenius relation $\tau_0 \exp(E^*/RT)$, where τ_0 is the pre-exponential factor and E^* the activation energy, the temperature of the endothermic peak, T_p, will be related to $\Delta H(t_a)$, or enthalpy lost on annealing, according to the equation

$$T_p^2 \propto \Delta H_a(t_a) \tag{4}$$

Since $\Delta H_a(t_a)$ is related to t_a by eq 3,

$$T_p^2 \propto \left\{1 - \exp\left[-\left(\frac{t_a}{\tau_a}\right)^{\beta}\right]\right\} \tag{5}$$

This means that a plot of T_p^2 vs the enthalpy lost will be a straight line with a positive slope, or that T_p^2 vs t_a or $\ln(t_a)$ will have the same shape as those of the loss of enthalpy vs t_a or $\ln(t_a)$. (The details of the derivation of eqs 4 and 5 and their implications for the mathematical modeling of the annealing behavior of polymers, as given in the literature, are beyond the scope of this paper and have therefore been excluded.) Plots of T_p^2 vs the enthalpy loss on annealing are shown in Figure 7b. This plot, which is for the sample containing 0.53 (g of water)/(g of NaDNA), shows that T_p^2 increases linearly with an increase in the enthalpy loss according to eq 4. According to the derivation of eq 4, which will be reported elsewhere, the constant of proportionality is $E^*/R[C_p(t_a) - (C_p(\infty)]$, where $C_p(t_a)$ refers to C_p after an annealing period of t_a and $C_p(\infty)$ after an infinitely long t_a. This quantity, which is equal to the slope of the line drawn in Figure 7b for the sample containing 0.53 (g of water)/(g of NaDNA), is equal to 7×10^3 g K^2 J^{-1}. If E^* is assumed to be 45 kJ mol^{-1}, which is about the energy required for the breaking of two H-bonds, as for water, $[C_p(t_a) - C_p(\infty)]$ is about 0.7 J g^{-1} K^{-1}, which seems very reasonable in view of the observation for other substances, e.g., diethyl phthalate,[42] for which the difference between a quenched sample (in fact cooled at 2.5 K/min) and an annealed sample was 0.01 J g^{-1} K^{-1}. For more rapidly cooled samples this difference increases by a large amount. It should be noted that eqs 3−5 describe how the first term of eqs 1 and 2 may be evaluated once β and τ_a are determined by experiments.

4. Effect of the Annealing Temperature. We now discuss the experimental determination of the second term of eqs 1 and 2 and of its implications for DNA's dynamics. When hydrated DNA is isothermally annealed for a fixed period, but at different

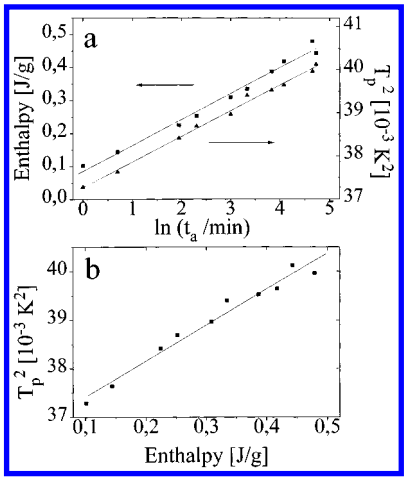

Figure 7. (a) Plots of recovered enthalpy in J/(g sample) and of the square of the peak maximum T_p^2 versus ln(annealing time) for various annealing periods at 183 K annealing temperature. (b) T_p^2, the square of the temperature at the peak maximum of the endothermic annealing effect, plotted as a function of the corresponding enthalpy for various annealing periods at 183 K annealing temperature. The water content of the sample was 0.53 (g of water)/(g of NaDNA). The annealing periods for (a) and (b) are those given in Figure 2.

annealing temperatures T_a, the area of the endotherm, or total ΔH_a observed on rate heating, increases up to a certain T_a and thereafter decreases, as seen in Figure 4. Ultimately, at a certain high temperature, this area becomes zero. The latter occurs only when the conformational substates are in their lowest energy at that temperature and the macroscopic state of the substance is in a thermodynamic equilibrium, i.e., the time needed to achieve the equilibrium being on the order of a few seconds or less. The temperature at which annealing does not cause an enthalpy decrease is the upper temperature limit of the glass transition endotherm or when the slowest mode of conformational motions has reached the equilibrium state in the substance. This temperature seems to be near 278 K for 0.46 (g water)/(g NaDNA), as the plots in Figure 4 indicate.

We first elaborate on why ΔH_a measured for a fixed t_a at increasing T_a reaches from zero to a peak value before becoming again zero. This is shown in Figure 8, which contains the results for both the enthalpy and entropy loss obtained for 0.46 (g of water)/(g of NaDNA). At a low T_a, the characteristic time τ_a of eq 3 for this relaxation is exceedingly long so that the decrease in H, or ΔH_a, is too small to be measurable. As T_a is increased, τ_a decreases rapidly according to the Arrhenius equation so that at each T_a there is a progressively larger decrease in H until the maximal value at $T_{a,max}$ is reached. Here, all the kinetically frozen in enthalpy has decreased within the period t_a, the DNA has lost its thermodynamic metastability, and its $H(\infty)$ value has been reached at $T_{a,max}$. Increasing T_a further but keeping t_a constant decreases both τ_a and $\Delta H_a(\infty)$ values at each temperature, i.e., equilibrium is attained in a progressively shorter time. Since $\Delta H_a(\infty)$, or the difference between $H(0)$ and $H(\infty)$, and $\Delta S_a(\infty)$, or the difference between $S(0)$ and $S(\infty)$, become vanishingly small at higher temperature, the two curves in parts a and b of Figure 6 come closer and meet at higher temperature, and the loss of the enthalpy and entropy on annealing, or $\Delta H_a(t_a)$ and $\Delta S_a(t_a)$, becomes zero. Thus, there are two processes, one that increases the enthalpy loss as T_a is increased and a second that decreases it. At low temperatures the first controls $\Delta H_a(t_a)$, and at high temperatures the second controls $\Delta H_a(t_a)$. The temperature at which the enthalpy loss reaches its maximum value is one from which the second effect begins to gain control of the annealing process of the DNA sample.

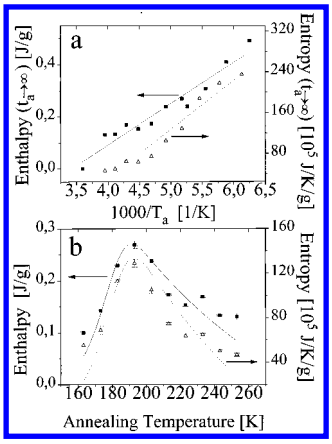

Figure 8. (a) Enthalpy and entropy losses at infinite annealing time $\Delta H(\infty)$ and $\Delta S(\infty)$ as a function of $1/T_a$ are shown for a sample containing 0.46 (g of water)/(g of NaDNA). Enthalpy and entropy values below 193 K are obtained from the extrapolated line of parts a and b of Figure 9. Above 193 K experimental enthalpy values from Figure 4 are used. In (b) the enthalpy and entropy losses of the same sample are shown as a function of annealing temperature for 20 min annealing time. The calculated lines are obtained for the enthalpy according to eq 6 with the parameters $\tau_0 = 3 \times 10^{-11}$ s, $E^* = 47$ kJ mol^{-1}, and $\beta = 0.6$ and for the entropy according to eq 9 with the parameters $\tau_0 = 3 \times 10^{-11}$ s, $E^* = 47.6$ kJ mol^{-1}, and $\beta = 0.6$.

Exact equations for describing this effect are complicated because of the fact that the equilibrium line or plot for $H(\infty)$ against T is itself curved, and this prevents us from a description of the phenomenon in terms of fictive temperature changes on annealing,[30] where the equilibrium line or plot for $H(\infty)$ against T is assumed to be linear. Phenomenologically, the process may be described by the equation

$$\Delta H_a(t_a,T_a) = \Delta H_a(\infty,T_a)[1 - \exp(-(t_a/\tau_a)^\beta)] \qquad (6)$$

where $\tau_a = \tau_0 \exp(E^*/RT_a)$, which is the Arrhenius equation, and $\Delta H_a(\infty,T_a)$ decreases with an increase in temperature. Derivation of conditions for which $\Delta H_a(t_a,T_a)$ will reach a maximum for fixed t_a but variable T_a gives T_p as the temperature for the endothermic peak maximum according to the equation

$$-\frac{\partial \ln \Delta H(\infty,T_a)}{\partial T_a} = \frac{\beta t_a^\beta E^*}{\tau_a^\beta R T_p^2} \qquad (7)$$

τ_a is the characteristic time at T_p calculated according to the Arrhenius equation $\tau_a = \tau_0 \exp(E^*/RT_p)$.

The magnitude of T_p is given by

$$T_p = \left[\frac{\beta t_a^\beta E^*}{-\tau_a^\beta R \dfrac{\partial \ln \Delta H(\infty,T_a)}{\partial T_a}}\right]^{1/2} \qquad (8)$$

τ_a depends on T_p and E^*. Thus, T_p or E^* can only be calculated by an iterative procedure or determined graphically if $\partial \ln \Delta H(\infty,T_a)/\partial T_a$ is known.

Here, t_a is not the isothermal annealing period as defined above, but it is the annealing time during continuous heating of the sample and can only be estimated as the time resolution of the DSC instrument. The plot for the enthalpy loss for hydrated NaDNA in Figure 9a gives $\partial \ln \Delta H_a(\infty)/\partial T_a = -0.0142$ K^{-1}. Using $\beta = 0.6$, $\tau_0 = 3 \times 10^{-11}$ s, $t_a = 0.8$ s (which is approximately the time resolution of the DSC instrument), $R = 8.314$ J mol^{-1} K^{-1}, and $T_p = 208.3$ K, we calculate $E^* \approx 46$ kJ mol^{-1}, which is consistent with the value of $E^* = 47$ kJ

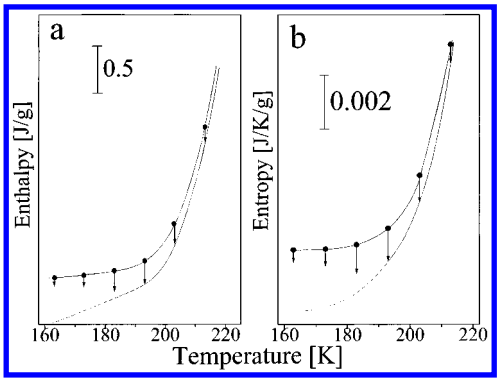

Figure 9. (a) Enthalpy and (b) entropy of a sample containing 0.46 (g water)/(g NaDNA) are plotted as a function of temperature. In addition the (a) enthalpy and (b) entropy losses during annealing at various annealing temperatures and 20 min annealing time are shown by the arrows. The dashed line is extrapolated for (a) enthalpy and for (b) entropy at infinite annealing time.

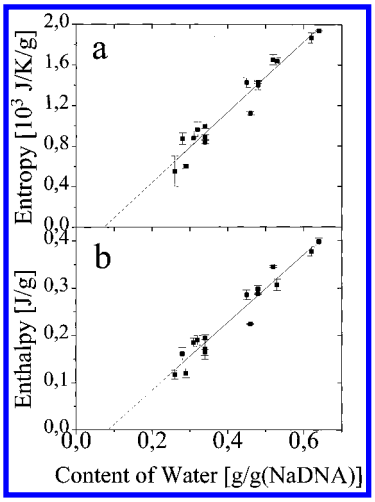

Figure 10. Entropy (a) and enthalpy (b) losses during annealing at 183 K for fixed annealing time of 20 min as a function of water content in (g of water)/(g of NaDNA). The straight line is obtained by linear regression. Extrapolation (dashed line) gives $\Gamma = 1.3$ for zero entropy recovery and $\Gamma = 1.5$ for zero enthalpy loss.

mol^{-1} calculated from the effect of annealing temperature on the enthalpy relaxation. The corresponding plot for the entropy loss in Figure 9b gives $\partial \ln \Delta S_a(\infty)/\partial T_a = -0.0198$ K^{-1}. Using $\beta = 0.6$, $t_a = 0.8$ s, $\tau_0 = 3 \times 10^{-11}$ s, and $T_p = 208.3$ K, we calculate $E^* \approx 45$ kJ mol^{-1}, which is approximately consistent with the value of $E^* = 47.6$ kJ mol^{-1} calculated from the effect of annealing temperature. This β and E^* value is for NaDNA with 0.48 (g of water)/(g of NaDNA) and $T_a = 183$ K obtained by evaluation of the data shown in ref 10 as Figure 3.

Equation 6 describes the measured enthalpy loss against t_a as well as T_a when the temperature dependence of $\Delta H_a(\infty)$ is known. The corresponding equation for the entropy decrease is

$$\Delta S_a(t_a,T_a) = \Delta S_a(\infty,T_a)[1 - \exp[-(t_a/\tau_a)^{\beta}]] \qquad (9)$$

where $\tau_a = \tau_0 \exp(E^*/RT_a)$ and all terms refer to the entropy (or enthalpy) loss on annealing. Since the value of $\beta = 0.6$ (with an estimated uncertainty of $\pm$ 0.1) is known for 0.48 (g of water)/(g of NaDNA) and $T_a = 183$ K (from Figure 3 in ref 10) and assuming that it does not vary with temperature, curves based on eqs 6 and 9 were calculated by first determining the functional form of $\Delta H_a(\infty)$ and $\Delta S_a(\infty)$ against T_a. Figure 8a shows that $\Delta H_a(\infty,T_a)$ increases linearly with the reciprocal temperature according to the equation $\Delta H_a(\infty,T_a) = -0.5455 + 159.3/T_a$, and $\Delta S_a(\infty,T_a)$ increases linearly with reciprocal temperature according to the equation $\Delta S_a(\infty,T_a) = -0.003525 + 0.95970/T_a$. By combining these values with eqs 6 and 9, $\Delta H_a(t_a,T_a)$ and $\Delta S_a(t_a,T_a)$ were calculated at various T_a for $t_a =$ 1200 s and the calculated curves are also plotted in Figure 8b. The remainder of the value needed to obtain the best fit of eqs 6 and 9 to the experimental data are $\tau_0 = 3 \times 10^{-11}$ s, $E^* = 47$ kJ mol^{-1}, and $\beta = 0.6$ for the enthalpy loss, and $\tau_0 = 3 \times 10^{-11}$ s, $E^* = 47.6$ kJ mol^{-1}, and $\beta = 0.6$ for the entropy loss. These values seem reasonable, since τ_0 is on the order of vibrational frequencies and E^* is about the same as required for breaking two H-bonds. They are consistent with the values obtained above (for enthalpy loss $E^* = 46$ kJ mol^{-1}, and for entropy loss $E^* = 47.6$ kJ mol^{-1}) for $T_p = 208.3$ K. The calculation of τ_a at 183.2 K with the obtained values from the enthalpy loss ($\tau_0 = 3 \times 10^{-11}$ s, $E^* = 47$ kJ mol^{-1}) gives $\tau_a =$ 13 min, which is comparable to $\tau_a = 19 \pm 5$ min determined from the time dependence of $\Delta H_a(t_a,T_a)$ (from Figure 3 in ref 10). This result justifies the assumption of the simple Arrhenius dependence of τ_a on T. In view of the experimental uncertainty and of the simplification by assuming that β remains constant with changing temperature, eqs 6 and 9 seem to describe adequately the enthalpy and entropy loss data of hydrated DNA.

5. Effect of Hydration on the Conformational Dynamics of DNA. We now discuss the physical significance of the third term in eqs 1 and 2. The temperature, T_p, at which the endotherm maximum appears for a constant heating rate after the same annealing conditions of different samples indicates the thermal energy at which the sample's relaxation time has reached a particular value, which in turn depends on the heating rate, β, and E^*. Alternatively stated, any procedure that lowers the T_p decreases the relaxation time of the molecular states that are mobile. Addition of water to NaDNA, as seen in Figure 1b, decreases T_p, and a plot of T_p vs water content in (g of water)/(g of NaDNA) (not shown) is nearly a straight line at water content above 0.26 (g of water)/(g of NaDNA).

Concurrently, the enthalpy and entropy losses on isothermal annealing at 183 K, which is measured from the area of the endotherms (including those shown in Figure 1b and additional ones), increase with increase of the water content of NaDNA, as shown in Figure 10. This indicates that the number of low-energy conformational states, which are attained after annealing for a fixed period, increases with an increase in the water content, or that hydrated DNA's mobility increases. It is remarkable that this increase occurs linearly with the increase in the water content as shown in Figure 10b, where the slope of the straight line is $(\partial \Delta H_a/\partial w)_{t_a,T_a} = 0.715$ J g^{-1}, and in Figure 10a, where the slope of the straight line is $(\partial \Delta S_a/\partial w)_{t_a,T_a} = 3.47 \times 10^{-3}$ J K^{-1} g^{-1}.

It is useful to consider whether or not the observed decrease in the relaxation time with increasing water content, as seen by a decrease in T_p and an increase in the enthalpy and entropy losses in Figure 10, is similar to the phenomenon known as plasticization of polymers. In the development of the phenomenology of molecular motions and thermodynamics of biopolymers, the change observed on increasing the water content may be seen as being effectively equivalent to an increase in the temperature of a sample of DNA with fixed water content. In doing so, we write

$$d\Delta H_a = \left(\frac{\partial \Delta H_a}{\partial w}\right)_{t_a,T_a} dw + \left(\frac{\partial \Delta H_a}{\partial T_a}\right)_{t_a,w} dT_a \qquad (10)$$

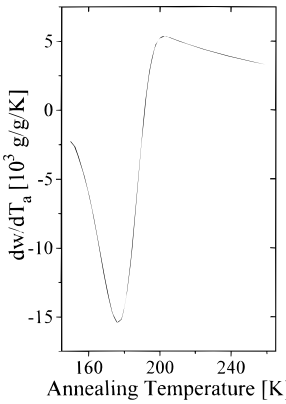

Figure 11. Plot of the change in the amount of water in (g of water)/(g of NaDNA) needed to have the same effect on the hydrated DNA's molecular kinetics as that caused by an increase or decrease in T_a, versus the annealing temperature. The annealing time was 20 min.

For the condition that $d\Delta H_a = 0$,

$$\left(\frac{\partial \Delta H_a}{\partial w}\right)_{t_a,T_a} dw = -\left(\frac{\partial \Delta H_a}{\partial T_a}\right)_{t_a,w} dT_a \qquad (11)$$

or

$$\left(\frac{\partial w}{\partial T_a}\right)_{t_a,\Delta H_a} = -\frac{(\partial \Delta H_a/\partial T_a)_{t_a,w}}{(\partial \Delta H_a/\partial w)_{t_a,T_a}} \qquad (12)$$

From Figure 10b, $(\partial \Delta H_a/\partial w)$ for a fixed t_a of 20 min at T_a = 183 K is 0.715 J g^{-1}. In Figure 8b $(\partial \Delta H_a/\partial T_a)$ is initially positive, becomes zero at 191 K, and thereafter becomes negative. Thus, $(\partial w/\partial T_a)_{t_a,\Delta H_a}$ from eq 12 is initially negative, becomes zero at 191 K, and thereafter becomes positive. $(\partial w/\partial T_a)_{t_a,\Delta H_a}$ was calculated from $(\partial \Delta H_a/\partial w)_{t_a,T_a} = 0.715$ J g^{-1} in Figure 10b and the calculated line in Figure 8b, and its value is plotted against the annealing temperature in Figure 11. This plot should be interpreted in terms of the change of the amount of water needed to have the same effect on the hydrated DNA's molecular kinetics as is caused by an increase in thermal energy after a 1 K rise in T_a. For example, at 175 K, $(\partial w/\partial T_a)_{t_a,\Delta H_a} = -0.015$ K^{-1}; i.e., a *decrease* by 0.015 (g water)/(g NaDNA) will accomplish the same change in the hydrated DNA's molecular kinetics, as measured by enthalpy relaxation, as a *decrease* in the annealing temperature by 1 K. At 191 K, where $(\partial w/\partial T_a)_{t_a,\Delta H_a}$ is equal to zero, an extremely small change in the amount of water has the same effect as a very large increase or decrease in the annealing temperature, i.e., the molecular kinetics in the vitrified 0.46 (g water)/(g NaDNA) is most sensitive to the change in the water content in the context of annealing kinetics. At annealing temperatures above 191 K, an *increase* in the water content has the same effect as a *decrease* in the annealing temperature, since $(\partial w/\partial T_a)_{t_a,\Delta H_a}$ remains positive. However, $(\partial w/\partial T_a)_{t_a,\Delta H_a}$ reaches a maximum positive value at 198 K, where the increase in the amount of water needed to cause the same effect as a 1 K rise in temperature is a maximum, at 0.005 (g water)/(g NaDNA). At the annealing temperature of 225 K only an increase by 0.004 (g water)/(g NaDNA) is required to have the same effect as a decrease by 1 K in T_a, since $(\partial w/\partial T_a)_{t_a,\Delta H_a}$ is now positive. Figure 11 thus describes a particularly important feature of the molecular activity or mobility of DNA, and by implication of proteins, since it provides an alternative to raising the temperature if there is a risk of irreversible chemical change in their structure on heating. More observations of a similar type on biological materials will be useful in ascertaining their stability in cryopreserved states.[43]

6. Effect of the Cooling Rate. An increase in the cooling rate increases the area of the endotherm caused by enthalpy recovery at a given T_a and a fixed t_a. This is shown in Figure 5 for a sample containing 0.50 (g of water)/(g of NaDNA) that has been annealed for 65 min at 183 K. For example, when this sample is annealed after cooling at 4 K min^{-1}, the recovered enthalpy is 0.21 J g^{-1}. It is 0.38 J g^{-1} after cooling at ~150 K min^{-1}, and it is 0.67 J g^{-1} after cooling at ~1500 K min^{-1}. The accompanying decrease in the endotherm's peak temperature from 201 to 200 K is marginal. In the process of vitrification, rapid cooling kinetically freezes in structural conformations of higher energies because the time scale at which the temperature changes is too short to allow attainment of their low-energy states. Thus, the enthalpy of a rapidly cooled vitrified hydrated DNA is greater than that of a slow cooled one. Thus, isothermal annealing of a rapidly cooled sample begins at a higher value of $H(0)$ than that of a slow cooled one, and so the decrease in the enthalpy over the same period is, for samples cooled at different rates, more when the cooling rate is high.

The increased magnitude of frozen-in enthalpy and entropy on cooling at high rates leads to a dilation or a decrease in the density of most glasses, with glassy water being an exception whose density increases with an increase in the rate of cooling.[44−46] Dilation usually reduces the relaxation time τ_a so that annealing occurs more rapidly (this is similar to the effect of lowering the pressure, which leads to dilation and reduction in the relaxation time). Thus, for the same annealing period t_a, the magnitude of ΔH_a and ΔS_a is greater when the frozen-in H and S are large. This seems to be a general observation for vitreous solids whose glass transition endotherm is relatively narrow[29,34,47] and for which a stretched exponential distribution of the structural relaxation times parameter β is used for analyzing the data, and this β is relatively large. But for a biomaterial, whose DSC endotherms lack a well-defined beginning and end, the data cannot be analyzed in terms of the parameter β. Hence, a description of the kinetic freezing of the molecular modes in DNA−H_2O on cooling and their unfreezing on heating in terms of a stretched exponential distribution of structural relaxation times remains unjustified. In this sense, the observation here of a larger magnitude of ΔH_a and ΔS_a, when the frozen-in H and S are large, is new and is worthy of further study.

Even higher cooling rates of up to ~10^6−10^7 K s^{-1} are used in cryofixation of biological specimens for cryoelectron microscopic studies with the aim to immobilize, or freeze in, the native state of dynamic structures and the momentary distribution of all components in a system.[48,49] Because of the extreme rates of cooling, the frozen-in H and S are even larger and τ_a even shorter. This leads to an enhanced mobility in the glassy state of hyperquenched aqueous solution and can be studied by changes in contact-ion pairing at temperatures as low as 100 K.[50] An FTIR spectroscopic study of the limits of cryofixation by using carbonylhemoglobin's CO conformer population as indicator and an analysis of the processes occurring during slow cooling and hyperquenching have been reported recently.[46]

7. Insights to Molecular Motions in DNA by Calorimetry. Irrespective of the nature of predominant interactions, intramolecular or intermolecular, that stabilize the various conformational substates, the heights of the barriers separating the substates are usually considered formally to be distributed between zero and infinity, as for example, in interpretations of results in terms of a stretched exponential response in terms of the parameter β. This leads to a relaxation time τ of the individual relaxation processes to range also from zero to

infinity. (Nevertheless, the ratio of relaxation times or the ratio of populations of the two substates in question at equilibrium is proportional to the exponential of the difference between the heights of two potential energy wells when the barrier heights between the two wells are finite.) In real systems τ neither approaches zero nor infinity, so there must be certain finite limits within which τ of a macromolecule can be considered to be distributed. Hence, it may be possible to envisage a biomolecule containing mobile elements that have different relaxation times at a fixed temperature, with the mobility of each being independent of each other, and the kinetics of the process of each has a single relaxation time. (It is noteworthy that in a recent paper on beef proteins, Sartor and Johari[51] have proposed a time dependent potential energy barrier picture with single relaxation times for protein segmental motions.) The reasons for the magnitude of β being less than unity may lie in the fact that, as discussed in section 1, the relaxation involves motions of several structural elements, each with its own single relaxation time, and thus a summation of several such relaxations leads to a decrease in the value of β from unity. It is also conceivable that the shape of the DSC scans in Figures 1 and 5 is a result of multiple processes whose β is less than unity but temperature dependent. Which of these explanations is satisfactory in terms of the apparent distribution of molecular relaxation rates requires further experiments and simulation of curves with a minimum number of *ad hoc* and adjustable parameters.

It is important to consider which part of the hydrated DNA molecule (or a water molecule itself) becomes kinetically frozen during vitrification on cooling and kinetically unfrozen on rate heating and at what temperature. In phenomenological descriptions of all vitrification processes this identification is ignored partly because the range of the glass transition of most synthetic polymers is narrow and partly because of the fact that there is no kinetic distinction between motions involving intra- and intermolecular degrees of freedom. (For example, the characteristics of the molecular kinetics of β- as well as α-relaxations in rigid molecular glasses without any intramolecular degrees of freedom have been known to be indistinguishable from the characteristics of the corresponding relaxations in amorphous polymers since 1970.[52]) Because of the need to understand such motions in vitrified hydrated DNA and proteins, it may be useful to develop techniques that could identify the molecular segments that lose their mobility on vitrification during cooling and that regain it on heating. We propose that one such technique is calorimetry. To use it, part of a segment of DNA may be deuterated and its DSC scan compared against the DSC scan of an undeuterated DNA measured under identical conditions. The temperature at which the two DSC scans show a difference will be the temperature at which the deuterated segment has become mobile. This would lead to the identification of the molecular entity. Isotopic substitution in various regions of a DNA and protein molecule would cause differences in the DSC scans of the normal and isotopically substituted macromolecule. With the accuracy currently available such experiments can be conveniently carried out.

Molecular processes observed at temperatures below ~220 K are thermally reversible over a narrow range of temperature and are relaxational in origin. Thus, the endothermic peak must be mainly associated with these molecular processes. However, it is conceivable that chemical reactions occur, and even with the resulting small decrease in enthalpy, they may distort the shape of the endotherm. But such a reaction will produce an exothermic feature because of a decrease in the enthalpy of chemical reaction, which will continue to high temperatures on rate heating. If the endotherm was superposed on this feature, it will either become vanishingly small or appear as an endothermic feature superposed on a very broad exotherm. This is not observed below ~220 and at 278 K but appears at temperatures between 213 and 263 K (see Figure 4, curves 7−10). At temperatures ≥278 K all molecular configurations are in their equilibrium state and no endothermic or exothermic effect is observed. Thus, we conclude that the first terms of eqs 1 and 2 contain contributions only from molecular processes up to temperatures of ~213 K. Above ~213 K, it contains contributions from physical processes and chemical reactions, and at ≥278 K, the term becomes zero as the equilibrium state is established.

Several recent studies have been interpreted to show that B-DNA is present at a certain temperature in the form of substates called B_I and B_{II}.[53] These two substates are in equilibrium at ambient and higher temperatures but are frozen in on the NMR time scale at 253 K.[54] If the B_I/B_{II} conformer population varies with temperature, then on rapid cooling a conformer population is frozen in at some temperature. Annealing at a lower temperature would cause kinetic unfreezing and attainment of the equilibrium conformer population. It is encouraging that the E^* value of 47 kJ mol^{-1} calculated here from the effect of annealing temperature is close to the mean barrier value of ~40 kJ mol^{-1} for the B_I/B_{II} transition reported in ref 53.

Acknowledgment. Financial support by the "Forschungsförderungsfonds" of Austria (Project P10404-PHY) is acknowledged.

References and Notes

(1) Frauenfelder, H.; Parak, F.; Young, R. D. *Annu. Rev. Biophys. Biophys. Chem.* **1988**, *17*, 451.
(2) Frauenfelder, H.; Sligar, S. G.; Wolynes, P. G. *Science* **1991**, *254*, 1598.
(3) Saenger, W. *Principles of Nucleic Acid Structure*; Springer: Berlin, 1984.
(4) McGammon, J. A.; Harvey, S. C. *Dynamics of proteins and nucleic acids*; Cambridge University Press: Cambridge, 1987.
(5) Kuwabara, T.; Mashimo, S.; Yagihara, S.; Umehara, S. *Biopolymers* **1990**, *30*, 649.
(6) Alam, T. D.; Drobny, G. P. *Chem. Rev.* **1991**, *91*, 1545.
(7) Gorenstein, D. G. *Chem. Rev.* **1994**, *94*, 1315.
(8) Jeffrey, G. A.; Saenger, W. *Hydrogen Bonding in Biological Structures*; Springer: Berlin, Heidelberg, New York, 1994.
(9) Berman, H. M. *Curr. Opin. Struct. Biol.* **1994**, *4*, 345.
(10) Rüdisser, S.; Hallbrucker, A.; Mayer, E. *J. Phys. Chem.* **1996**, *100*, 458.
(11) Sartor, G.; Mayer, E.; Johari, G. P. *Biophys. J.* **1994**, *66*, 249.
(12) Green, J. L.; Fan, J.; Angell, C. A. *J. Phys. Chem.* **1994**, *98*, 13780.
(13) Miyazaki, Y.; Matsuo, T.; Suga, H. *Chem. Phys. Lett.* **1993**, *213*, 303.
(14) Rupley, J. A.; Careri, G. *Adv. Protein Chem.* **1991**, *41*, 37.
(15) Breslauer, K. J.; Freire, E.; Straume, M. *Methods Enzymol.* **1992**, *211*, 533.
(16) Sartor, G.; Mayer, E.; Johari, G. P. *J. Polym. Sci., Part B: Polym. Phys.* **1994**, *32*, 683.
(17) Kuntz, I. D., Jr.; Kauzmann, W. *Adv. Protein Chem.* **1974**, *28*, 239.
(18) Mrevlishvili, G. M. *Sov. Phys. Usp.* **1979**, *22*, 433. Andronikashvili, E. L.; Mrevlishvili, G. M.; Japaridze, G. Sh.; Sokhadze, V. M.; Tatishvili, D. A. *J. Non-Equilib. Thermodyn.* **1989**, *14*, 23.
(19) Pissis, P. *J. Mol. Liq.* **1989**, *41*, 271.
(20) Laudat, J.; Laudat, F. *Europhys. Lett.* **1992**, *20*, 663.
(21) Kurinou, I. V.; Krypyanskii, Yu. F.; Panchenko, A. R.; Suzdalev, I. P.; Uporov, I. V.; Shaitan, K. V.; Rubin, A. B.; Goldanskii, V. I. *Hyperfine Interact.* **1990**, *58*, 2355.
(22) Taillandier, E.; Liquier, J.; Taboury, J. A. In *Advances in Infrared and Raman Spectroscopy*; Clark, R. J. H., Hester, R. E., Eds.; Heyden: London, 1985; Vol. 12, Chapter 2.
(23) Falk, M.; Hartman, K. A., Jr.; Lord, R. C. *J. Am. Chem. Soc.* **1962**, *84*, 3843.
(24) Falk, M.; Hartman, K. A., Jr.; Lord, R. C. *J. Am. Chem. Soc.* **1963**, *85*, 387.
(25) Falk, M.; Hartman, K. A., Jr.; Lord, R. C. *J. Am. Chem. Soc.* **1963**, *85*, 391.

(26) Wolf, B.; Hanlon, S. *Biochemistry* **1975**, *14*, 1661.
(27) Lindsay, S. M.; Lee, S. A.; Powell, J. W.; Weidlich, T.; Demarco, C.; Lewen, G. D.; Tao, N. J.; Rupprecht, A. *Biopolymers* **1988**, *27*, 1015.
(28) Sartor, G.; Hallbrucker, A.; Mayer, E. *Biophys. J.* **1995**, *69*, 2679.
(29) Hodge, I. M. *J. Non-Cryst. Solids* **1994**, *169*, 211.
(30) Hodge, I. M.; Berens, A. R. *Macromolecules* **1982**, *15*, 762.
(31) Cavaille, J. Y.; Perez, J.; Johari, G. P. *Phys. Rev. B* **1989**, *39*, 2411.
(32) Perez, J. *PHYSIQUE ET MECANIQUE DES POLYMERES AMORPHES*; Lavoisier, Tec & Doc: Paris, 1992.
(33) Scherer, G. W. *J. Am. Ceram. Soc.* **1984**, *67*, 504.
(34) Scherer, G. W. *RELAXATION IN GLASS AND COMPOSITES*; John Wiley: New York, 1986.
(35) Rekhson, S. M. *J. Non-Cryst. Solids* **1986**, *84*, 68.
(36) Kovacs, A. J.; Aklonis, J. J.; Hutchinson, J. M.; Ramos, A. R. *J. Polym. Sci., Part B: Polym. Phys.* **1979**, *17*, 1097.
(37) Hofer, K.; Mayer, E.; Hodge, I. M. *J. Non-Cryst. Solids* **1992**, *139*, 78.
(38) Lagasse, R. R. *J. Polym. Sci., Part B: Polym. Phys.* **1982**, *20*, 279.
(39) Fransson, A.; Bäckström, G. *Int. J. Thermophys.* **1987**, *8*, 351.
(40) Mountain, R. D.; Thirumalai, D. *J. Chem. Phys.* **1990**, *92*, 6116.
(41) Stephens, R. B. *J. Non-Cryst. Solids* **1976**, *20*, 75.
(42) Chang, S. S.; Horman, J. A.; Bestul, A. B. *J. Res. Natl. Bur. Stand.* **1967**, *A71*, 293.
(43) Potts, M. *Microbiol. Rev.* **1994**, *58*, 755.
(44) Angell, C. A. *Annu. Rev. Phys. Chem.* **1983**, *34*, 593.
(45) Johari, G. P.; Fleissner, G.; Hallbrucker, A.; Mayer, E. *J. Phys. Chem.* **1994**, *98*, 4719.
(46) Mayer, E. *J. Am. Chem. Soc.* **1994**, *116*, 10571.
(47) Kauzmann, W. *Chem. Rev.* **1948**, *43*, 219.
(48) Plattner, H.; Bachmann, L. *Int. Rev. Cytol.* **1982**, *79*, 237.
(49) Dubochet, J.; Adrian, M.; Chang, J.-J.; Homo, J. C.; Lepault, J.; McDowall, A. W.; Schultz, P. *Q. Rev. Biophys.* **1988**, *21*, 129.
(50) Fleissner, G.; Hallbrucker, A.; Mayer, E. *J. Phys. Chem.* **1995**, *99*, 8401.
(51) Sartor, G.; Johari, G. P. *J. Phys. Chem.* **1996**, *100*, 10450.
(52) Johari, G. P.; Goldstein, M. *J. Chem. Phys.* **1970**, *53*, 2372.
(53) Hartmann, B.; Piazzola, D.; Lavery, R. *Nucleic Acids Res.* **1993**, *21*, 561.
(54) DiVerdi, J. A.; Opella, S. J. *J. Mol. Biol.* **1981**, *149*, 307.